Boundary and impurity effects on the entanglement of Heisenberg chains

Xiaoguang Wang

Australian Centre of Excellence for Quantum Computer Technology, Department of Physics, Macquarie University,
Sydney, New South Wales 2109, Australia
and Zhejiang Institute of Modern Physics, Zhejiang University, Hangzhou 310027, China
(Received 15 December 2003; published 10 June 2004)

We study entanglement of a pair of qubits and the bipartite entanglement between the pair and the rest within open-ended Heisenberg *XXX* and *XY* models. The open boundary condition leads to strong oscillations of entanglements with a two-site period, and the two kinds of entanglements are 180° out of phase with each other. The mean pairwise entanglement and ground-state energy per site in the *XXX* model are found to be proportional to each other. We study the effects of a single bulk impurity on entanglement, and find that there exist threshold values of the relative coupling strength between the impurity and its nearest neighbors, after which the impurity becomes pairwise entangled with its nearest neighbors.

I. INTRODUCTION

Over the past few years much effort has been put into studying quantum entanglement in various quantum spin models. At zero temperature, entanglement naturally exists in many-body ground states. The systems contain two classes, finite spin clusters [1–18] such as a ring of qubits, and infinite spin systems [19–26], where quantum phase transition [27] may occur. For a ring of qubits interacting via the Heisenberg *XXX* Hamiltonian, the ground-state concurrence, quantifying entanglement of a pair of qubits, is equal to the absolute value of the ground-state energy per site [2,9]. Universal scaling behaviors of quantum entanglement of ground states emerge at a quantum phase transition point in the anisotropic *XY* model [19–21]. Experimentally, the entangled state of magnetic dipoles has been found to be crucial to describing magnetic behaviors in a quantum spin system [28].

In most of the previous studies on entanglement of many-body ground states, a periodic boundary condition (PBC) is assumed for spin chains. In compounds such as Mn_{12} and Fe_8, the metal ions within a single molecule form almost a perfect ring, which can be described by the Heisenberg interaction [29]. On the other hand, spin chains with an open boundary condition (OBC) have been used to construct spin cluster qubits [30,31] for quantum computation and employed for quantum communication from one end to another [32,33]. Perfect state transfer has been obtained via the open chain without requiring qubit coupling to be switched on and off [33]. These investigations reveal that open chains are of great advantage in implementing quantum information tasks. Thus the study of the entanglement structure in open spin chains will be of importance as the entanglement underlies operations of quantum computing and quantum information processing. Here, we investigate open boundary effects on ground-state entanglement. We also note a recent study of quantum entanglement in the *XXZ* model in the presence of domain walls [34], which can be considered as a kind of OBC.

A linear open *N*-qubit chain can be viewed as a ring of (*N*+1)-qubit chains with an impurity [(*N*+1)th qubit], where

the coupling $J_{N+1,1}=J_{N+1,N}=0$. The impurity plays a very important role in condensed matter physics, and it will be interesting to see its effect on quantum entanglement. In earlier studies, impurity effects on entanglement have been considered with a three-spin small system [35]. Here, we consider large spin systems described by the Heisenberg *XY* model.

The paper is organized as follows. In Sec. II A, by exact diagonlization method, we study the ground-state entanglement in the Heisenberg *XXX* model with an OBC. The mean nearest-neighbor entanglement is found be proportional to the ground-state energy per site. For studying systems with a large number of sites, in Sec. II B we consider the *XY* model with an OBC, which can be solved exactly by Jordan-Wigner mapping [35]. Entanglements display strong oscillations over lattice. With increase of the ground-state energy, the mean pairwise entanglement increases in the *XY* model, while it decreases in the *XXX* model. In Sec. III, we study impurity effects on entanglement of the spin systems described by the *XY* model, where the impurity is located in the bulk of the system. We conclude in Sec. IV.

II. BOUNDARY EFFECTS

A. Heisenberg *XXX* model

We consider a physical model of *N* qubits interacting via the isotropic Heisenberg Hamiltonian with an OBC,

$$H_{XXX} = \frac{J}{2}\sum_{i=1}^{L-1}(1 + \sigma_{ix}\sigma_{i+1x} + \sigma_{iy}\sigma_{i+1y} + \sigma_{iz}\sigma_{i+1z}), \quad (1)$$

where $\vec{\sigma}_i=(\sigma_{ix},\sigma_{iy},\sigma_{iz})$ is the vector of Pauli matrices and *J* is the exchange constants. The positive and negative *J* correspond to the antiferromagnetic (AFM) and ferromagnetic (FM) case, respectively.

The SU(2) symmetry ($[H,S_\alpha]=0$) is evident, where $S_\alpha=\Sigma_{i=1}^N \sigma_{i\alpha}/2, \alpha \in \{x,y,z\}$. This symmetry guarantees that reduced density matrix ρ_{ij} of two qubits, say qubit *i* and *j*, for the ground state ρ has the form [2]
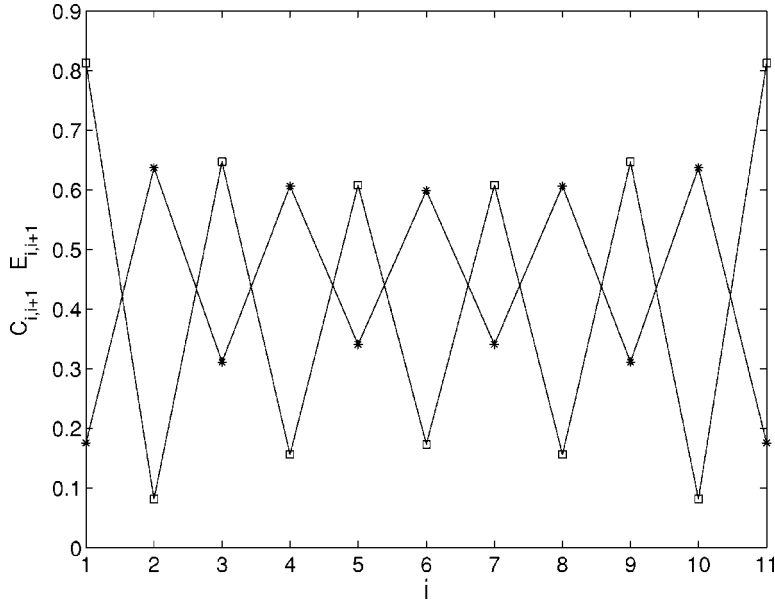
FIG. 1. Ground-state nearest-neighbor concurrence (square line) and linear entropy (star line) versus site number for $L=12$ in the Heisenberg *XXX* model.

$$\rho_{ij} = \begin{pmatrix} u_{ij} & 0 & 0 & 0 \\ 0 & w_{ij} & z_{ij} & 0 \\ 0 & z_{ij} & w_{ij} & 0 \\ 0 & 0 & 0 & u_{ij} \end{pmatrix} \qquad (2)$$

in the standard basis $\{|00\rangle,|01\rangle,|10\rangle,|11\rangle\}$.

From the reduced density matrix, the concurrence [37] quantifying the entanglement is readily obtained as [2,9]

$$C_{i,j} = 2 \max[0,|z_{ij}| - u_{ij}] = \max[0,|G_{i,j}^{xx}| - G_{i,j}^{zz}/2 - 1/2]$$
$$= \max(0,|G_{ij}^{zz}| - G_{ij}^{zz}/2 - 1/2) = \max(0,-3G_{ij}^{zz}/2 - 1/2),$$
$$(3)$$

where $G_{ij}^{\alpha\alpha}=\text{Tr}(\sigma_{1\alpha}\sigma_{2\alpha}\rho)$ are correlation functions. The second equality follows from the relations between matrix elements of ρ_{ij} and correlation functions given by $u_{ij}=(1+G_{ij}^{zz})/4$ and $z_{ij}=G_{ij}^{xx}/2$. The SU(2) symmetry leads to the third equality. The fourth equality follows from the inequality $|G_{ij}^{zz}| \leq 1$, which is a special case of a more general result that $|\langle A\rangle| \leq 1$ for any Hermitian operator A satisfying $A^2=1$. We see that the qubits i and j are entangled if $G_{ij}^{zz}<-1/3$.

For studying bipartite entanglement, we consider an even number of sites, for which ground states of the Heisenberg model are nondegenerate, and thus pure. The bipartite entanglement of pure states is well defined by entropies of one subsystem. Here, for convenience, we choose the linear entropy to quantify the bipartite entanglement between a pair of qubits and the rest. From Eq. (2), in a similar way to get Eq. (3), the linear entropy for ρ_{ij} is obtained as

$$E_{ij} = 1 - \text{Tr}(\rho_{ij}^2) = 1 - \tfrac{1}{4}[1 + 3(G_{ij}^{zz})^2]. \qquad (4)$$

The reduced density matrix ρ_{ij} is only determined by the correlation function G_{ij}^{zz}, as is the concurrence and the linear entropy.

Due to the nearest-neighbor nature of the interaction in our system, the entanglement between a pair of nearest qubits is expected to be prominent compared with a pair of non-nearest-neighbor qubits. Thus we focus on the nearest-neighbor case in the following discussions. For the isotropic Heisenberg Hamitonian with a PBC, entanglements between qubits i and $i+1$ are independent on index i. However, for the case of OBC, the concurrence C_{ii+1} and the linear entropy E_{ii+1} must be site dependent due to the breaking of translational symmetry. Next, we study entanglements using the exact diagonalization method.

We first diagonalize Hamitonian H_{XXX} to obtain the ground state, from which we calculate the correlation function G_{ii+1}^{zz}, and then the pairwise and bipartite entanglements via Eqs. (3) and (4), respectively. The numerical results for 12 qubits (4069-dimensional Hibert space) are shown in Fig. 1. The entanglements oscillate with a two-site period, and the concurrence and the linear entropy are 180° out of phase with each other. The pair with qubits 1 and 2, and the one with qubits $L-1$ and L, display maximal pairwise entanglement (minimal bipartite entanglement). For two qubits interacting via the Heisenberg Hamiltonian, they prefer the maximally entangled singlet state $|\Psi\rangle=(1/\sqrt{2})(|01\rangle-|10\rangle)$ with concurrence $C=1$. Qubit 1 favors maximal entanglement with the only nearest-neighbor qubit 2, and results in higher concurrence C_{12}. For qubit 2, there is a competition between qubits 1 and 3, and they both favor being maximally entangled with qubit 2. Qubit 2 shares a large entanglement with qubit 1, and thus results in less entanglement with qubit 3, and the oscillatory feature appears. As the pair of qubits 1 and 2 have a strong entanglement, the bipartite entanglement between the pair of qubits with the rest of the system is relatively suppressed as we have seen from the figure.

It will be instructive to give two extreme examples to reveal relations between pairwise entanglement and the biparite entanglement between the pair and the rest. The first one is the singlet state with $C=1$ and $E=0$, and the second one is the maximally mixed state $\rho_{12} = \text{diag}(1/4,1/4,1/4,1/4)$ with $C=0$ and $E=0.75$ (maximal
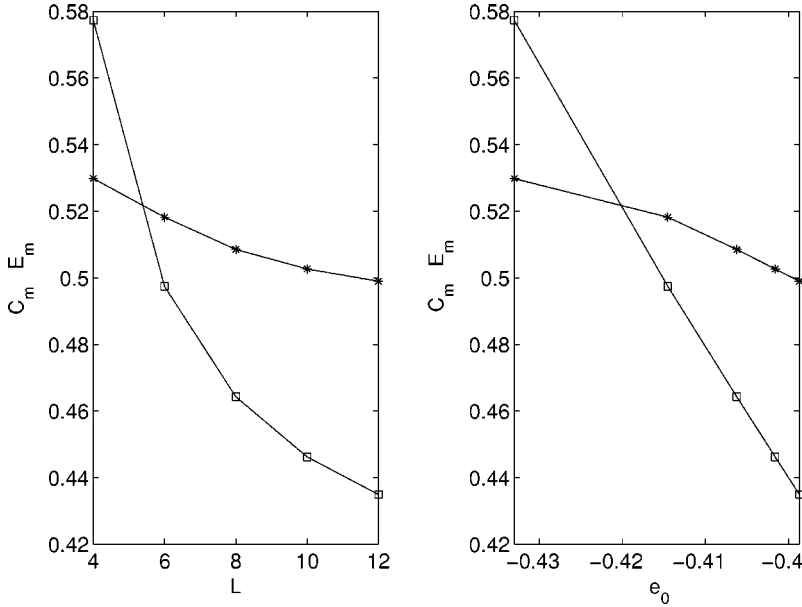
FIG. 2. Mean concurrence (square line) and mean linear entropy (star line) versus L and e_0 in the Heisenberg *XXX* model.

linear entropy). Thus, in general, the above numerical results and the two simple examples suggest that the more the pairwise entanglement, the less the bipartite entanglement. Of course, this is not a general statement for arbitrary multiqubit states.

Next, we consider the mean entanglement and study its relations with ground-state energy $\mathcal{E}_0$. The nearest-neighbor mean concurrence and linear entropy can be defined as

$$C_m(L) \equiv \frac{1}{L-1} \sum_{i=1}^{L-1} C_{i,i+1},$$

$$E_m(L) \equiv \frac{1}{L-1} \sum_{i=1}^{L-1} E_{i,i+1}. \qquad (5)$$

We made numerical calculations for even L from 4 to 12, and the entanglements versus L or e_0 are shown in Fig. 2, where $e_0 = \mathcal{E}_0/L$ is the ground-state energy per site. The pairwise entanglement decreases as L or e_0 increases, and so does the bipartite entanglement. More interestingly, the pairwise entanglement decreases linearly with e_0. We may obtain an analytical relation between C_m and e_0 as follows.

The numerical results for the finite lattices show that $C_{ii+1} > 0$, and thus from Eq. (3) we obtain

$$G_{ii+1}^{zz} = \frac{-2C_{ii+1} - 1}{3}. \qquad (6)$$

From H_{XXX} (1) and after taking into account the SU(2) symmetry, we get

$$e_0 = \frac{L-1}{2L} + \frac{3}{2L} \sum_{i=1}^{L-1} G_{ii+1}^{zz}. \qquad (7)$$

Substituting Eq. (6) into Eq. (7) leads to

$$e_0 = -\frac{L-1}{L} C_m(L), \qquad (8)$$

where we have used the definition of mean concurrence. The above relation shows that the mean entanglement is proportional to the ground-state energy per site, implying that less energy gives more pairwise entanglement. Although this relation is obtained for finite lattices, we make a conjecture that it is valid for any number of lattice sites.

The concurrence and linear entropy obtained for finite sites of lattice up to 12 are not so close to those for infinite lattice given by

$$C_m(\infty) = 2 \ln 2 - 1 \approx 0.3863,$$

$$E_m(\infty) = \tfrac{2}{3}[1 - \ln 2(2 \ln 2 - 1)] \approx 0.4882. \qquad (9)$$

This is due to the finiteness of lattice, and also due to the effects of boundaries. To investigate effects of open boundaries on entanglement in *larger* systems, we next study the quantum Heisenberg *XY* model, which can be solved exactly by the Jordan-Wigner transformation [36].

B. Heisenberg *XY* model

The Heisenberg *XY* Hamiltonian with an OBC is given by

$$H_{XY} = \frac{J}{2} \sum_{i=1}^{N-1} (\sigma_{ix}\sigma_{i+1x} + \sigma_{iy}\sigma_{i+1y}). \qquad (10)$$

There are two symmetries in the Hamiltonian. One is a U(1) symmetry ($[H, S_z] = 0$), and another is a Z_2 symmetry ($[H, \Sigma_x] = 0$), where $\Sigma_x = \sigma_{1x} \otimes \sigma_{2x} \otimes \cdots \otimes \sigma_{Nx}$. They guarantee that reduced density matrix ρ_{ij} of two qubits i and j for the ground state ρ is given by Eq. (2). For the lack of SU(2) symmetry, the correlation functions G_{ij}^{zz} and G_{ij}^{xx} are no longer equal, and then the concurrence is given by

$$C_{ij} = \max[0, |G_{ij}^{xx}| - G_{ij}^{zz}/2 - 1/2], \qquad (11)$$

determined by two correlation functions.

For the nearest-neighbor cases, two correlation functions G_{ii+1}^{xx} and G_{ii+1}^{zz} are dependent, and the latter can be written in terms of the former as we will see shortly, and thus the concurrence is only determined by a single correction function G_{ii+1}^{xx}. To show this, we use the well-known Jordan-Wigner mapping $\sigma_i^+ \mapsto c_i^\dagger \Pi_{k=1}^{i-1} \exp(i\pi c_k^\dagger c_k)$ [36], under which Hamiltonian H_{XY} *exactly* maps to

$$H_{XY} = J \sum_{i=1}^{L-1} (c_i^\dagger c_{i+1} + c_{i+1}^\dagger c_i) \qquad (12)$$

due to the OBC, where c_i and $c_i^\dagger$ are Fermionic annihilation and creation operators, respectively. Then, in the Fermionic representation, the two correlation functions can be written as

$$z_{ii+1} = \langle c_i^\dagger c_{i+1} \rangle,$$

$$u_{ii+1} = \langle c_i^\dagger c_i c_{i+1}^\dagger c_{i+1} \rangle = 1/4 - |\langle c_i^\dagger c_{i+1} \rangle|^2, \qquad (13)$$

where we have used the Wick theorem [38], and the fact that $\langle c_i^\dagger c_i \rangle = 1/2$ for any i. Thus the concurrence is determined only by one correlation function $\langle c_i^\dagger c_{i+1} \rangle$,

$$C_{ii+1} = 2 \max(0, |\langle c_i^\dagger c_{i+1} \rangle| + \langle c_i^\dagger c_{i+1} \rangle^2 - 1/4). \qquad (14)$$

To compute the correlation function $\langle c_i^\dagger c_{i+1} \rangle$, we first diagonalize the Hamiltonian H_{XY} by the following transformation:

$$c_n = \sum_{k=1}^{L} g_{nk} \widetilde{c}_k = \sqrt{\frac{2}{L+1}} \sum_{k=1}^{L} \sin\left(\frac{nk\pi}{L+1}\right) \widetilde{c}_k. \qquad (15)$$

After the transformation, the Hamiltonian H_{XY} can be written as

$$H_{XY} = \sum_{k=1}^{L} \epsilon_k \widetilde{c}_k^\dagger \widetilde{c}_k = \sum_{k=1}^{L} -2 \cos\left(\frac{k\pi}{L+1}\right) \widetilde{c}_k^\dagger \widetilde{c}_k, \qquad (16)$$

where ϵ_i is the single-particle energy, and $J=-1$ is assumed for convenience. The ground state is then expressed as

$$|\Psi\rangle_{GS} = \widetilde{c}_1^\dagger \widetilde{c}_2^\dagger, \dots, \widetilde{c}_{L/2}^\dagger |0\rangle, \qquad (17)$$

with energy $\mathcal{E}_0 = \Sigma_{k=1}^{L/2} \epsilon_k$. From the above expression of the ground state, the correlation function is obtained as

$$\langle c_i^\dagger c_{i+1} \rangle = \sum_{k=1}^{L/2} g_{i,k} g_{i+1,k}. \qquad (18)$$

The combination of Eqs. (14) and (18) gives an exact analytical expression for the concurrence. By using Eq. (13), the linear entropy of the two-qubit reduced density matrix ρ_{ii+1} is obtained as
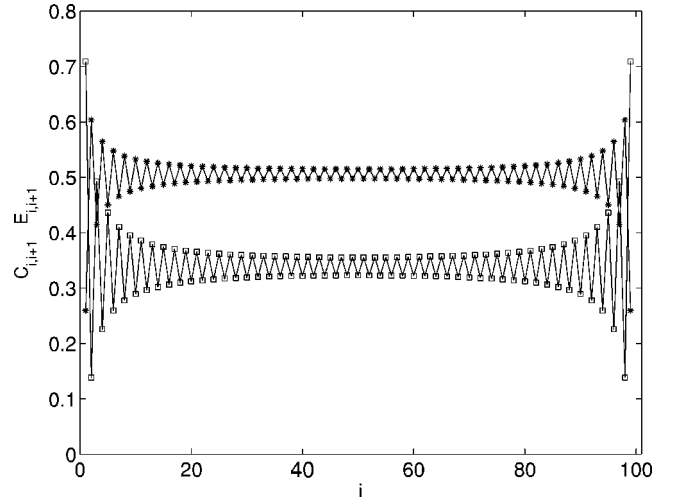

FIG. 3. Ground-state nearest-neighbor concurrence (square line) and linear entropy (circle line) entanglement versus site number for $L=100$ in the Heisenberg *XY* model.

$$E_{ii+1} = 3/4 - 4|\langle c_i^\dagger c_{i+1} \rangle|^4 - 2|\langle c_i^\dagger c_{i+1} \rangle|^2, \qquad (19)$$

which is also analytical. From these analytical expressions, entanglements are readily calculated numerically for a very large L.

Figure 3 displays features of entanglement distribution over lattice sites, which are similar to those of the Heisenberg *XXX* model. Strong oscillations of entanglements are more evident. The similarity arises since two qubits interacting via the Heisenberg *XY* interaction also favor the singlet state. Near the bulk area, the entanglements oscillate with nearly the same amplitude with respect to the mean value, and the boundary effects diminish.

Now, we study the mean entanglements for different L. Figure 4 gives the entanglement versus L and the energy per site. With the increase of L, the mean concurrence decreases, while the linear entropy increases, and both saturate for large L. For a infinite lattice, the concurrence and the linear entropy are given by

$$C_m(\infty) = \frac{2}{\pi} + \frac{2}{\pi^2} - \frac{1}{2} \approx 0.3393,$$

$$E_m(\infty) = \frac{3}{4} - \frac{4}{\pi^4} - \frac{2}{\pi^2} \approx 0.5063. \qquad (20)$$

We see that the concurrence and linear entropy with $L=200$ are nearly identical to those with infinite L. From Fig. 4, we observe that the mean concurrence increases, while the mean linear entropy decreases with the increase of energy. The behavior of the mean concurrence is opposite to that in the Heisenberg *XXX* model. Here, the lower energy does not correspond to higher pairwise entanglement.

III. IMPURITY EFFECTS

As we have stated in the Introduction, a linear open N-qubit chain can be viewed as a ring of $(N+1)$-qubit chains
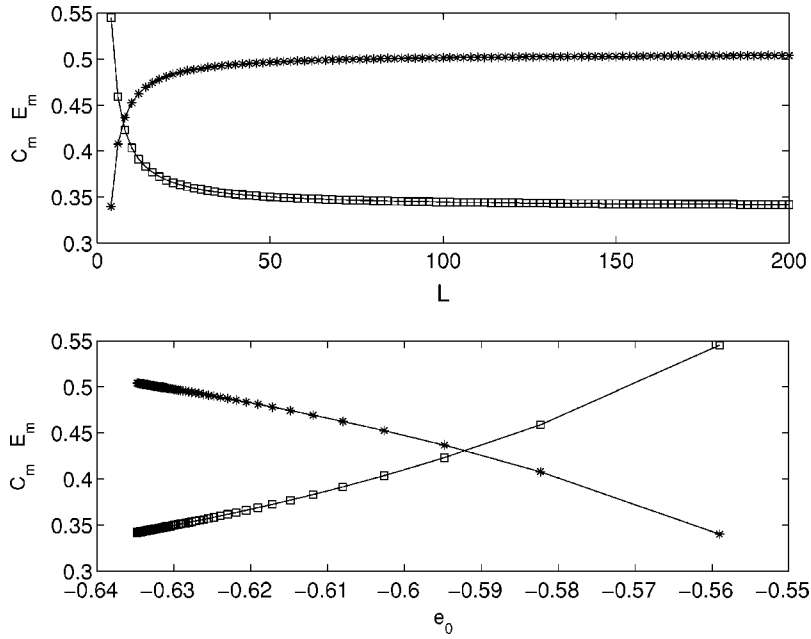
FIG. 4. Mean concurrence (square line) and mean linear entropy (star line) versus L and e_0 in the Heisenberg XY model.

with an impurity. In this section, we study single impurity effects on the entanglement of Heisenberg chains. We consider the Heisenberg XY model described by the Hamiltonian

$$H_{XY} = \sum_{i=1}^{N-1} \frac{J_{i,i+1}}{2} (\sigma_{ix}\sigma_{i+1x} + \sigma_{iy}\sigma_{i+1y}) \qquad (21)$$

with an OBC. Now, we assume that the single impurity spin is located in the bulk (site $N/2$) [39], namely,

$$J_{N/2-1,N/2} = J_{N/2,N/2+1} = J' = \alpha J,$$

$$J_{i,i+1} = J = 1 \text{ for other } i, \qquad (22)$$

where α characterizes the relative strength of the coupling between the impurity qubit and its nearest neighbors. To be specific, we focus on pairwise entanglement in the following discussions.

Due to the existence of a single impurity in the bulk, we do not expect analytical results for entanglement. However, the Hamiltonian still has the U(1) and Z_2 symmetries, so we can map the Hamiltonian exactly to a Fermionic one, and the Wick theorem applies. Thus Eqs. (11) and (14) for the concurrence are valid and applicable to the impurity model. All
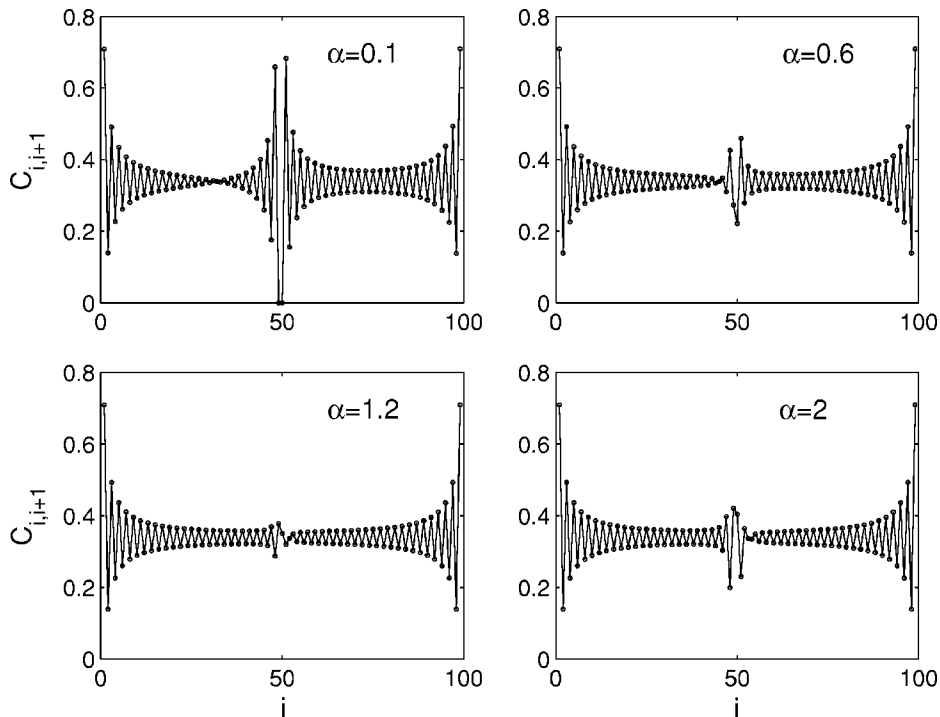

FIG. 5. Ground-state nearest-neighbor concurrence versus site number for $L=100$ in the Heisenberg XY model with an impurity.
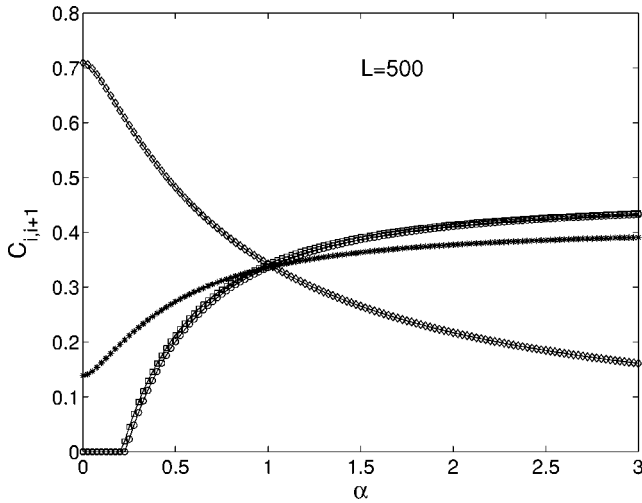
FIG. 6. Ground-state nearest-neighbor concurrences $C_{N/2-1,N/2}$ (square line), $C_{N/2,N/2+1}$ (circle line), $C_{N/2+1,N/2+2}$ (diamond line), and $C_{N/2+2,N/2+3}$ (star line), as a function of α for the impurity model.

we need is to diagonalize a $L \times L$ matrix to obtain the coefficients g_{nk} in the expression $c_n = \Sigma_{k=1}^{L} g_{nk} \tilde{c}_k$, and then calculate the correlation function $\langle c_i^{\dagger} c_{i+1} \rangle$ via the relation $\langle c_i^{\dagger} c_{i+1} \rangle = \Sigma_{k=1}^{L/2} g_{ik}^{*} g_{i+1,k}$. Note that the summation is from $k=1$ to $L/2$ since the system considered is nondegenerate (the single-particle energy ϵ_k is not zero) and number of the negative values of ϵ_k are $L/2$.

From Fig. 5, we see that the impurity leads to additional oscillations of the pariwise entanglement in the bulk region. For small $\alpha=0.1$, the concurrences $C_{N/2-1,N/2}$ and $C_{N/2,N/2+1}$ are zero. Even the coupling between the impurity qubit and its nearest neighbors are not zero, the entanglement between them vanishes due to competition among qubits. For larger $\alpha=0.6$, the entanglements between impurity qubit and qubits $L/2+1$ and $L/2-1$ build up, where $C_{N/2-1,N/2} > C_{N/2,N/2-1}$, which also holds for $\alpha=1.2>1$ and $\alpha=2>1$. The difference between the two concurrences results from the choice of even N, leading to a nonsymmetry of the entanglement distribution. We see that even one single impurity has strong effects on entanglement structure, especially in the region near the impurity.

From the above analyses, it is expected that there exists a threshold value of α, after which the impurity qubit and its nearest neighbors becomes entangled. In Fig. 6, we plot the nearest-neighbor concurrences in the bulk region as a function of α. It is evident that there exist threshold values α_1 for concurrence $C_{N/2-1,N/2}$ and α_2 for concurrence $C_{N/2,N/2+1}$. The

threshold value α_2 is slightly larger than α_1, and the pairwise entanglement between the impurity and qubit $N/2-1$ is always a little stronger than that between the impurity and qubit $N/2+1$ when $\alpha > \alpha_2$. We also observe that the increase of α suppresses the concurrence $C_{N/2+1,N/2+2}$, while it enhances the concurrence $C_{N/2+2,N/2+3}$. When $\alpha=1$ (no impurity case), all concurrences shown in the figure are almost identical since we have chosen a large $L=500$, which diminishes the boundary effects in the bulk and the amplitudes of oscillations become very small.

IV. CONCLUSION

In conclusion, we have studied ground-state entanglements in Heisenberg *XXX* and *XY* models with an OBC. The OBC leads to strong oscillations with a two-site period of entanglement in a pair of nearest-neighbor qubits and bipartite entanglement between the pair and the rest. The maximal pairwise entanglement and minimal bipartite entanglement occurs at open ends, and the two kinds of entanglements are 180° out of phase with each other. In both models, the two-qubit reduced density matrix is determined by only one correlation function, and so do the entanglements. We have found that the mean entanglement is proportional to the ground-state energy per site in the *XXX* model. With increase of the ground-state energy, the mean pairwise entanglement decreases in the *XXX* model, while it increases in the *XY* model.

We study the effects of a single bulk impurity on entanglement, and find that the impurity leads to additional oscillations of entanglement in the bulk region. We also find that there exists threshold values of the relative coupling strength between the impurity and its nearest neighbors, after which the impurity becomes entangled with its nearest neighbors. As the entanglement underlies operations of quantum computation and quantum information processing, the structures of entanglement found in the present studies are useful when we make a simulation of quantum systems where boundary and impurity effects cannot be negligible. Inside a quantum computer, a quantum register could be an open chain with around 100 qubits, for which, as we have shown within the Heisenberg *XY* model, the boundary effects are still significant in the bulk. It deserves to make further studies of boundary effects on a real quantum computer.

[1] M. A. Nielsen, e-print quant-ph/0011036, Ph.D. thesis, University of Mexico, 1998.

[2] K. M. O'Connor and W. K. Wootters, Phys. Rev. A **63**, 052302 (2001).

[3] M. C. Arnesen, S. Bose, and V. Vedral, Phys. Rev. Lett. **87**, 017901 (2001).

[4] X. Wang, Phys. Rev. A **64**, 012313 (2001); **66**, 034302 (2002); Phys. Lett. A **281**, 101 (2001).

[5] D. Gunlycke, V. M. Kendon, V. Vedral, and S. Bose, Phys. Rev. A **64**, 042302 (2001).

[6] X. Wang, H. Fu, and A. I. Solomon, J. Phys. A **34**, 11 307 (2001).

[7] G. L. Kamta and A. F. Starace, Phys. Rev. Lett. **88**, 107901 (2002).

[8] Y. Yeo, Phys. Rev. A **66**, 062312 (2002).

[9] X. Wang and P. Zanardi, Phys. Lett. A **301**, 1 (2002); X. Wang, Phys. Rev. A **66**, 044305 (2002).

[10] Y. Sun, Y. Chen, and H. Chen, Phys. Rev. A **68**, 044301 (2003).

[11] L. Zhou, H. S. Song, Y. Q. Guo, and C. Li, Phys. Rev. A **68**, 024301 (2003).

[12] A. Saguia and M. S. Sarandy, Phys. Rev. A **67**, 012315 (2003).

[13] J. Schliemann, Phys. Rev. A **68**, 012309 (2003).

[14] D. A. Meyer and N. R. Wallach, J. Math. Phys. **43**, 4273 (2002).

[15] O. F. Syljuåsen, Phys. Rev. A **68**, 060301(R) (2003).

[16] L. F. Santos, Phys. Rev. A **67**, 062306 (2003).

[17] U. Glaser, H. Büttner, and H. Fehske, Phys. Rev. A **68**, 032318 (2003).

[18] T. Meyer, U. V. Poulsen, K. Eckert, M. Lewenstein, and D. Bruss, e-print quant-ph/0308082.

[19] T. J. Osborne and M. A. Nielsen, Phys. Rev. A **66**, 032110 (2002).

[20] A. Osterloh, L. Amico, G. Falci, and R. Fazio, Nature (London) **416**, 608 (2002); L. Amico, A. Osterloh, F. Plastina, R. Fazio, and G. M. Palma, Phys. Rev. A **69**, 022304 (2004).

[21] G. Vidal, J. I. Latorre, E. Rico, and A. Kitaev, Phys. Rev. Lett. **90**, 227902 (2003); J. L. Latorre, E. Rico, and G. Vidal, Quantum Inf. Comput. **4**, 48 (2004).

[22] I. Bose and E. Chattopadhyay, Phys. Rev. A **66**, 062320 (2002).

[23] J. Vidal, G. Palacios, and R. Mosseri, Phys. Rev. A **69**, 022107 (2004).

[24] S. J. Gu, H. Q. Lin, and Y. Q. Li, Phys. Rev. A **68**, 042330 (2003).

[25] O. Osenda, Z. Huang, and S. Kais, Phys. Rev. A **67**, 062321 (2003).

[26] B. Q. Jin and V. E. Korepin, e-print quant-ph/0304108.

[27] S. Sachdev, *Quantum Phase Transitions* (Cambridge University Press, Cambridge, England, 2000).

[28] S. Ghosh, T. F. Rosenbaum, G. Aeppli, and S. N. Coppersmith, Nature (London) **425**, 48 (2003).

[29] See, for instance, O. Waldmann, Phys. Rev. B **65**, 024424 (2002).

[30] F. Meier, J. Levy, and D. Loss, Phys. Rev. Lett. **90**, 047901 (2003).

[31] F. Meier, J. Levy, and D. Loss, Phys. Rev. B **68**, 134417 (2003).

[32] S. Bose, Phys. Rev. Lett. **91**, 207901 (2003); V. Subrahmanyam, Phys. Rev. A **69**, 034304 (2004).

[33] M. Christandl, N. Datta, A. Ekert, and A. J. Landahl, Phys. Rev. Lett. **92**, 187902 (2004).

[34] F. C. Alcaraz, A. Saguia, M. S. Sarandy, e-print quant-ph/0312039.

[35] H. Fu, A. I. Solomon, and X. Wang, J. Phys. A **35**, 4293 (2002); X. Q. Xi, S. R. Hao, W. X. Chen, and R. H. Yue, Phys. Lett. A **297**, 291 (2002).

[36] P. Jordan and E. Wigner, Z. Phys. **47**, 631 (1928); E. Lieb, T. Schultz, and D. Mattis, Ann. Phys. (N.Y.) **16**, 407 (1961).

[37] W. K. Wootters, Phys. Rev. Lett. **80**, 2245 (1998).

[38] G. C. Wick, Phys. Rev. **80**, 268 (1950).

[39] J. Stolze and M. Vogel, Phys. Rev. B **61**, 4026 (2000).